Manuscript title

Investigation the interrelation between soil mechanical characteristics and unsaturated hydraulic conductivity curve using tension disc infiltration

Authors name and affiliations:

Azadeh Sedaghat[1, *], Hossein Bayat[2], and Seyed Majid Mousavi[3]

1- Department of Irrigation and Soil Physics; Soil and Water Research Institute; Agricultural Research, Education and Extension Organization (AREEO); 3177993545 Karaj; Iran
2- Department of Soil Science; Faculty of Agriculture; Bu-Ali Sina University; Hamedan; Iran
3- Department of Soil Fertility and Plant Nutrition; Soil and Water Research Institute; Agricultural Research, Education and Extension Organization (AREEO); 3177993545 Karaj; Iran

***Corresponding Author:**
A. Sedaghat (azadehsedaghat65@gmail.com)

ABSTRACT

Soil compaction reduces the yield of agricultural products. Due to the problems of drought and the low amount of organic matter in the soil of Iran, soil compaction is one of the important problems in Iran's agriculture. Hydraulic conductivity is sensitive to compaction created in the soil and generally decreases with compaction as a function of soil water content. Considering the local variation in soil hydrological characteristics and the a lack of efficient in-situ measuring tools, evaluating these features at the field scale is challenging. Pedotransfer functions (PTFs) can be used to solve this problem. Thus, this study aims to use soil mechanical characteristics for parametric estimation of the field scale unsaturated hydraulic conductivity curve (K curve). Four Iranian provinces' lands were sampled for 105 soil samples. The samples were mostly taken from areas with a conservation tillage system. K was determined in the field using a tension disc infiltrometer. It was also estimated using the Gardner model (1958) by 16 PTFs. To estimate the K, a combination of new factors and methods of ANN (Artificial Neural Network) and MLR (Multiple Linear Regression) was used. The K curve was estimated using the factors of the CC curve (Confined Compression curve) and other soil characteristics. In the MLR method, the lowest IRMSE (0.73) value was found at level 7 in the training step, which used the basic soil characteristics, along with the Gompertz model coefficient as predictors in comparison with the level one (RMSE=1.4) which used only the basic characteristics of soil as predictors. In addition, in the testing step, level 5 with the inputs of the soil basic characteristics along with the factors modified of the Van Genuchten model by Baumgartl and Kock (2004) ($VG_{modified}$) had the best results and decreased the IRMSE from 1.03 in the first step to 0.68. Generally, PTF10 with the input of penetration resistance, along with the basic soil characteristics, had the best result in both steps. The PTF_{10}, decreased the AIC from 949 (PTF_1) to 377 in the training step and from

464 (PTF_1) to -150 in the testing step. In general, it is concluded that there is a good correlation between the K curve and the soil's mechanical characteristics.

Keywords: Confined Compression; Gardner model; Parametric pedotransfer functions; Tension disc infiltration; Unsaturated hydraulic conductivity.

1. Introduction

Hydraulic conductivity at and near saturation condition (K_s and K) are among the most important characteristics defining water behavior in the soil (Báťková et al., 2020). The K curve is defined as a function of moisture or suction (Bayat et al., 2015). For sustainable management of water resources and agricultural land, it is essential to establish the hydraulic and hydro-dispersive characteristics of the soil (Dragonetti et al., 2022). To examine seasonal or temporal variability within a crop cycle, or between sample dates of different crop years, several sampling times are required because soil hydraulic characteristics are extremely changeable in both location and time (Kreiselmeier et al., 2020; Castellini et al., 2019). However, K measurement can be a time-and-cost-consuming process (Van Genuchten, 1980). Some in situ techniques, such as the tension disc infiltrometer, have been designed primarily to determine K in the field (Angulo-Jaramillo et al., 2000). Tension disc infiltration is a K-based direct measurement method with a short time, wide data availability, and easy application (Li et al., 2018).

The soil CC curve illustrates the connection between the applied stress logarithm and the void ratio (Keller et al., 2011). Keller et al. (2011) described the swelling or recompression index (Cs), compressibility coefficient or compression index (Cc), and pre-consolidation or pre-compression

stress (Pc), as three significant factors that were retrieved from the soil CC curve. In contrast to Cc, which is characterized by plastic deformations and is irreversible, Cs is used to determine rebound and soil mechanical resilience. (Keller et al., 2011). Pc is the mathematical term used to describe the boundary between the elastic and plastic parts of the CC curve (Casagrande, 1936).

Moreover, due to the heterogeneity of soil, hydraulic conductivity in a field is highly spatially varied, and several measurements are required to determine it. Therefore, it is important to develop faster and cheaper methods for determining the soil's hydraulic factors (Ali, 2018). As an alternative to measurements,estimation methods that utilize physical or empirical relations between hydraulic characteristics and other soil variables can be used. The advantage of such methods, which are known as pedotransfer functions (PTF_s), is that the input variables can be determined more easily and, hence, are more widely available than hydraulic characteristics. For the estimation of water retention and saturated and K, this approach has led to several PTF_s that use soil texture, bulk density (BD) (Bayat et al., 2015; Lin et al., 2014; Azadmard et al., 2020), or other soil variables as inputs (Sedaghat et al., 2022). Therefore, it is important to develop alternative, rapid, and inexpensive methods to estimate these characteristics to keep research active (Patil and Singh, 2016).In the last few decades, regression methods and data mining techniques have been widely used to create PTFs (Adab et al., 2020; Gunarathna et al., 2019).

Bayat et al. (2015) reported several similarities between the K and the CC curve. Therefore, due to the similarity of the two curves, it seems likely that the same factors, such as texture, structure, BD, soil moisture, clay, and OM affect both curves. As opposed to the time-consuming and difficult process of determining the K curve, the CC curve can be determined relatively easily (Moustafa, 2000). According to An et al. (2015), Cc decreases with high BD, and its value is reduced when a combination of high BD and low soil moisture is used. According to Baumgartl and Köck (2004), these processes are significantly influenced by hydraulic conductivity (textural factor) and soil permeability (physicochemical factors).

According to the analysis of the CC curves in this study, it was determined that moisture content affected the CC curve shape more than the initial void index or BD. Compaction of wet soil results in the deformation of air-filled pores within the soil matrix, which leads to re-arrangements in porosity (between macropores and micropores), and changes in volume. This condition is related to several soil characteristics and stresses (Wiermann et al., 2000).

Bayat et al. (2015) examined the connection between the CC and K curves and estimated K using the van Genuchten-Mualem model. However, in this research, K was determined with a tension disc infiltrometer under field conditions and was simulated using the Gardner model. According to literature reviews, no one has estimated K under field conditions using the compression behavior of soil. Finding the connection among these characteristics would be a great step forward in the estimation of the K curve for the field conditions. Therefore, investigating the parametric estimation of the K curve with tension disc infiltration in the field is the aim of this study, through the factors of the Gardner model using CC curve factors.

2. Materials and methods

2.1. Soils

Samples of disturbed and undisturbed soil were collected for this study from 105 locations of West Azarbaijan (12 samples; 44º3´, 47º23´ N; 35º8´, 39º46´ E), East Azarbaijan (12 samples; 45º5´, 189 48º22´ N; 36º45´, 39º26´ E), Hamedan (69 samples; 47º48´, 49º28´ N; 34º00´, 35º44´ E) and Kermanshah (12 samples; 45º24´,48º06´ N; 33º41´, 35º17´ E) provinces of Iran. The samples were mostly taken from areas with conservation tillage systems. The sampling depth from 0 to 35 cm. The distribution of the sampling points is shown in Fig. 1. Table 1 summarizes some of the features

of the soil sampling locations. Samples of undisturbed soil were collected using cylinders with a diameter of 5.4 cm and height of 4.8 cm.

Table 1. Features of the soil sampling site

	Taxonomy	Total rainfall (mm/year)
West Azarbaijan	Inceptisols, Entisols	600
East Azarbaijan	Inceptisols, Entisols	210.1
Hamedan	Inceptisols, Entisols	300
Kermanshah	Entisols, Vertisols, Inceptisols, and Mollisols	445

Physical and mechanical characteristics of the soil samples were determined (Table 2). The soil texture was determined using the method of Gee and Or (2002). The BD was determined using the cylinder method (Grossman and Reinsch, 2002). With the use of the Brazilian technique, the TS of aggregates was determined (Dexter and Kroesbergen, 1985).

Table 2. Description of the factors

Factors	Description	Unit
C	Clay	(%)
Si/Sa	Silt/Sand	-
BD	Bulk density	g/cm^3
θ_{sv}	Saturated volumetric moisture	% v/v
CEC	Cation exchange capacity	meq/100 gr
Ts	Tensile strength	kPa
PR	Penetration resistance	kPa
P_c	Pre-compaction stress	kPa
C_c	Compression index	1/log kPa
C_s	Swelling index	1/log kPa
e	Void ratio is equal to any applied stress	cm^3/ cm^3
e_0	Initial void ratio	cm^3/ cm^3
e_{25}	Void ratio at 25 kPa stress	cm^3/ cm^3
e_s	Void ratio before stress application	cm^3/ cm^3
e_r	Minimum void ratio	cm^3/ cm^3
a		
b	Gompertz model coefficient	-
c		

m		
α^* n^*	Factors modified of Van Genuchten model by Baumgartl and Kock (2004) ($VG_{modified}$)	1/log kPa
σ_i	Stress at inflection point	kPa
σ_{mc}	Stress at maximum curvature	kPa
α	Shape factor of the Gardner model	cm/h
K_0	Hydraulic conductivity at zero suction	cm/h
K	Unsaturation hydraulic conductivity	cm/h

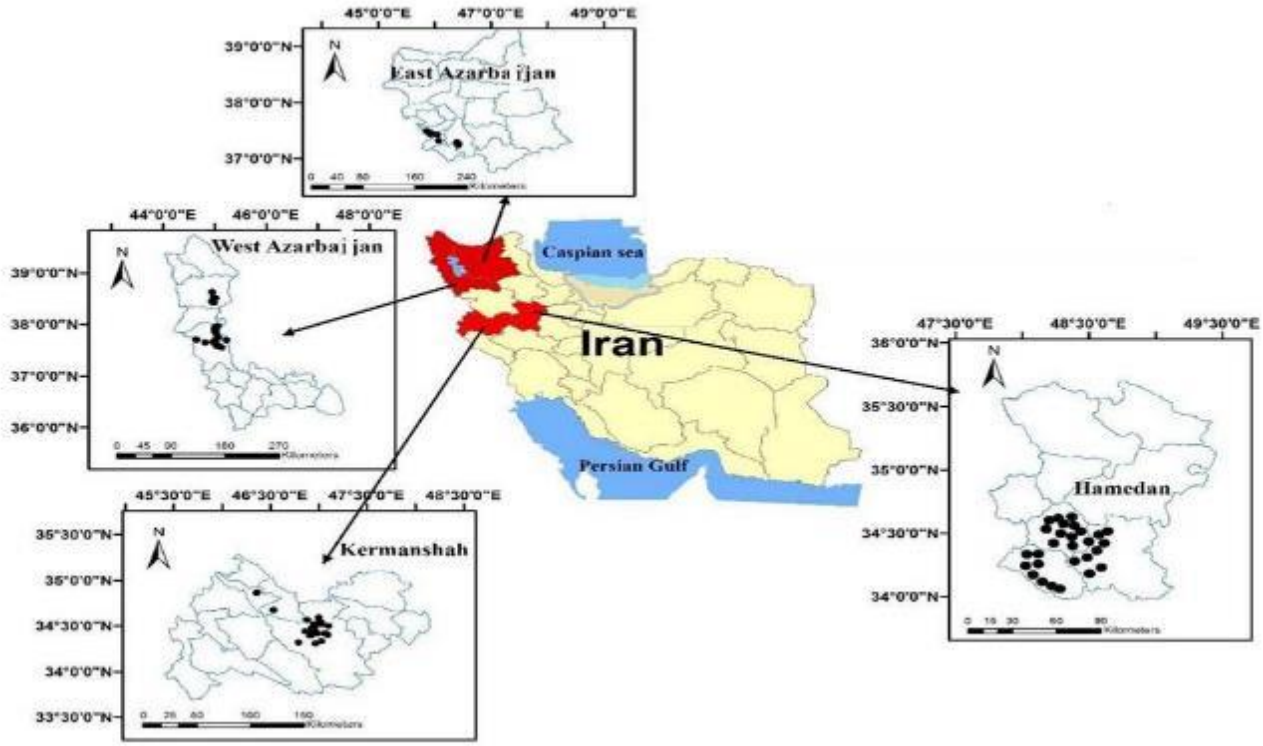

Fig. 1. Map of the sampling zone

2.2. Confined compression test

The confined compression test (CCT) uses a uniaxial system (California Bearing Ratio). To perform CCT, in a pressure plate apparatus, undisturbed samples were set to matric suction at 100 kPa. The loading and unloading phases were conducted during this test. A CBR cylinder device

was used to load the samples at a maximum loading speed of 1000 kPa (mm/min). 33 readings were taken at a distance 0.03 (mm) in the unloading step (Koolen, 1974). Another gage was used at the same time as the imposed stresses to determine the height reduction (H) in the soil samples caused by the applied stress. Eq. 1 was used to determine the volume change (or void ratio) for every stress. After CCT, the soil samples were dried in an oven at 105°C for 48 h (Koolen and Kuipers, 1989).

$$\frac{\Delta H}{H} = \frac{\Delta e}{1+e_0} \qquad e = e_0 - \Delta e \qquad \text{Eq.1}$$

where the soil sample's initial height is H (cm), the void ratio change is Δe (cm^3/ cm^3), and the sample height change is ΔH (cm).

2.2.1 Confined compression curve

2.2.1.1. Gompertz model (1825)

On the basis of the confined compression loading data, Solver optimizer software (Excel, 2013) modified the Gompertz model (1825) (Eq. 2). Using the Gompertz model coefficients (1825), the C_c factor by Eq. 3 and the C_s factor by Eq. 4 were calculated. Casagrande's graphical method (1936) was used to obtain the P_c factor:

$$e = a + c\exp\left\{-\exp\left[b(\log\sigma - m)\right]\right\} \qquad \text{Eq.2}$$

Approximately, the value of "a" is equal to e_0, "m" is equal to log σ_i, and C_c is equal to σ_{mc} (Gregory et al., 2006).

$$C_c = \frac{bc}{\exp(1)} \quad \text{Eq.3}$$

The mean slope of the loading path up to 25 kPa of stress was used to calculate the Cs factor (Keller et al., 2011) as follows:

$$C_{s\,Loadin-25kPa} = \frac{e_0 - e_{25kPa}}{\log(25kPa)} \quad \text{Eq.4}$$

2.2.1.2. The $VG_{modified}$ model by Baumgartl and Kock (2004)

According to the report of Baumgartl and Kock (2004), the van Genuchten (1980) model was modified on the basis of mechanical factors to obtain the total void ratio–stress model (Eq. 5). Solver optimization software (Excel, 2013) was used to derive the coefficients *, n*, and m* of $VG_{modified}$ model.

$$\frac{e - e_r}{e_s - e_r} = \left[1 + (\alpha^* \sigma)^{n^*}\right]^{-m^*} \quad \text{Eq.5}$$

The factors of Eq. 5 are described in Table 2. The minimum void ratio e_r is generally around 0.27. The CC curve factors of α^* and m^* were used to calculate the factors of σ_i (Eq. 6) and σ_{mc} (Eq. 7)

$$\sigma_i = 10^{x_i} = 1/(1/m^*)^{1/n*} \quad \text{Eq.6}$$

$$\sigma_{mc} = \frac{1}{\alpha^*} Y_{mc}^{1/n^*} = \frac{1}{\alpha^*}\left(\frac{3m^* + 1 - \sqrt{5m^{*2} + 6m^* + 1}}{2m^{*2}}\right)^{1/n*} \quad \text{Eq.7}$$

2.3. **Methods with tension disc infiltration**

To determine the hydraulic conductivity in the field, a disc infiltration with a disk diameter of 20 (cm) was used. The test was performed from higher to lower matrix suction. The tests were conducted in two matric suction of 10 and 5 cm. Data gathering continued until reaching a constant water diffusion in the soil at least matrix suction. Immediately after the end of the experiments, the soil under the disk was sampled to determine the final moisture content. Using the multi-potential method, to determine the saturated hydraulic conductivity (Perroux and White, 1988), infiltration measurements were realized for two different tension values and interpreted using Wooding's method (Wooding, 1968).

2.3.1. **Fit the tension disc infiltration (Wooding (1968) and Gardner model (1958))**

Factor α of Gardner (1958) (i.e., the slope of K versus matric suction), and the saturated hydraulic conductivity (K_0) using the Wooding model (1968) (Eq.8) and the exponential equation of Gardner (1958) (Eq.9- 12) were calculated as follows:

$$Q(h) = \pi R^2 K \left[1 + \frac{4}{\pi R \alpha} \right] \quad \text{Eq.8}$$

$$K(h) = K_0 \exp(\alpha h) \quad \text{Eq.9}$$

where h is the suction (cm) applied to the device and R is the pore radius (cm). By combining Equations 8 and 9, the volumetric flow rate for two different suction h_1 and h_2 is obtained, and the following equations are obtained:

$$Q(h_1) = \pi R^2 K_0 \exp(\alpha h_1) \left[1 + \frac{4}{\pi R \alpha} \right] \quad \text{Eq.10}$$

$$Q(h_2) = \pi R^2 K_0 \exp(\alpha h_2)\left[1 + \frac{4}{\pi R \alpha}\right] \quad \text{Eq.11}$$

By combining equations 10 and 11, the factor α is obtained as follows:

$$\alpha = \frac{\ln\left[Q(h_2)/Q(h_1)\right]}{h_2 - h_1} \quad \text{Eq.12}$$

K_0 is calculated by placing "α" factor in equations 10 and 11.

2.4. Developing pedotransfer functions

The preprocessing process involved detecting outliers, performing normality tests, and using multicollinearity and residual independence tests applied to all factors (Al-Jabery et al., 2019). Data outliers were determined using the interquartile range (IQR) method (Seo, 2006). The Kolmogorov-Smirnov normality test was performed using MiniTab software for all variables, and the variables that did have not normal distribution were transformed (Liu et al., 2020). All variables have been standardized to have a variance of 1 and a mean of 0. In each of the six groups, 53 and 52 samples were chosen at random for the training and testing steps, respectively. The Si/Sa ratio was used in the PTFs to prevent multicollinearity. All PTFs underwent a multicollinearity test using the variance inflation factor criterion (VIF). The VIF is calculated using Eq. 13 (Marquaridt, 1970):

$$\mathrm{VIF} = \frac{1}{1 - \mathrm{R}_i^2} \quad \text{Eq.13}$$

Where, R_i^2: a coefficient of determination for a regression model that is unadjusted the i^{th}, and the variables are independent of one another. The VIF of PTFs should not be higher than 10, which is generally used to detect multicollinearity, and this method can be used to detect multicollinearity (Ho, 2006). In this study, the VIF values for all 16 levels were evaluated, and all were below 10 (results not shown). Multiple linear regression (MLR) using DataFit software and artificial neural networks (ANN) using STATISTICA12 software were used to create PTFs.

In this study, to estimate K, models were created using MLP (Multilayer Perceptron) (Agyare et al., 2007) and RBF (Radial Basis Functions) (Picton, 2000; Amini et al., 2005) networks. This network differs significantly from the MLP network in terms of the expression for the input to the RBF in the second layer. In this study, the performances of two different ANN types were assessed; for each type, a single hidden layer and numerous hidden neurons (Between three to twenty), were used. The highest degree of accuracy and reliability was attained by testing various transfer functions, including tanh, exponential, logistic, identity, and sine in the hidden and output layers.

2.5. Description of the models

Input variables were used to estimate the Gardner model factors (α and K_0). In this study, inputs were categorized into six groups according to their similarities (Table 3). The factors of the Gardner model (1958) (α and K_0) were estimated by the two methods, and then K was calculated using the Gardner model. Fig. 2 represents the thorough procedure for using the Gardner model to estimate the K curve.

Table 3. Using input variables to estimate Gardner model factors (α and K0).

PTFs	Group	Input variables
PTF_1	1	C^a, Si/Sa, BD

PTF_2	2	C, Si/Sa, BD, P_c, C_c, C_s
PTF_3		C, Si/Sa, BD,±
PTF_4		C, Si/Sa, BD, σ_i, σ_{mc}
PTF_5	3	C, Si/Sa, BD, α^*, n^*
PTF_6		C, Si/Sa, BD, α^*, n^*, e_0
PTF_7		C, Si/Sa, BD, a, b, c, m
PTF_8		C, Si/Sa, BD, ±
PTF_9	4	C, Si/Sa, BD, Ts
PTF_{10}		C, Si/Sa, BD, PR
PTF_{11}	5	C, Si/Sa, BD, CEC
PTF_{12}		C, Si/Sa, BD, θ_{sv}
PTF_{13}	6	P_c, C_c, C_s
PTF_{14}		a, b, c, m
PTF_{15}		α^*, n^*, e_0
PTF_{16}		σ_i, σ_{mc}

± The inputs for PTF_3 and PTF_8 were those variables that had the strongest correlation with the output variables. For instance, in the PTF_3 the Cc has the highest correlation with Gardener's α and K_0 factors, and in the PTF_8 the coefficients a, m, and c, a Gampartz model, are used to estimate the factors α and K_0, respectively.

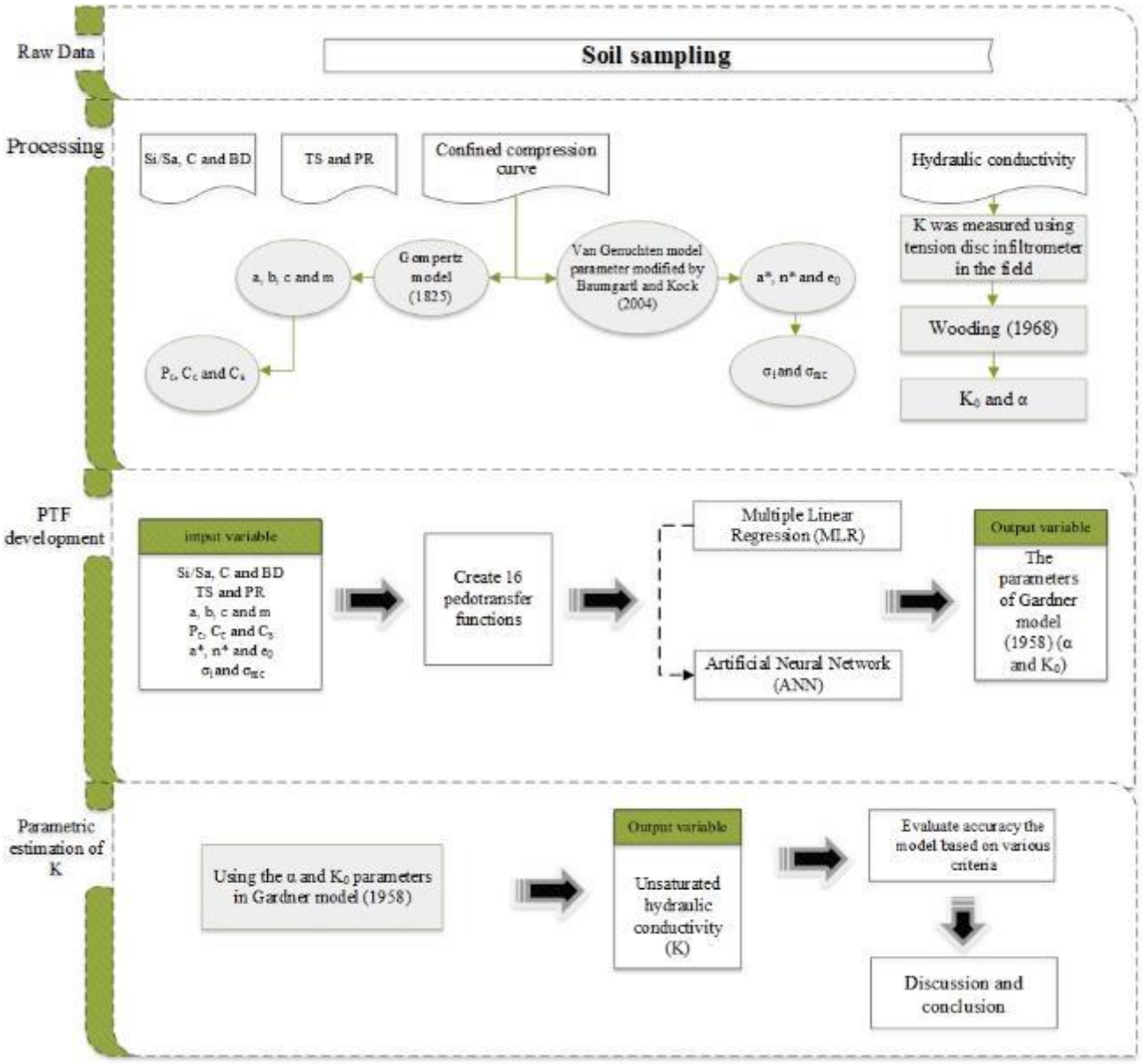

Fig. 2. Detailed process of estimating the K curve using the Gardner model

2.6. Evaluation criteria

Some criteria, including AIC (Akaike's information criterion) (Akaike, 1974), R^2 (Coefficient of determination), RI (Relative Improvement), IRMSE (Integral Root Mean Square Error), and IME (Integral Mean Error), were used to investigate the estimation accuracy of SM using the two methods, as follows:

$$AIC = N \ln\left[\sum_{i=1}^{N} \frac{(y_i - \hat{y}_i)^2}{N}\right] + 2n_p \quad \text{Eq.13}$$

$$R^2 = 1 - \frac{\sum_{1}^{N}\left(y_i - \hat{y}_i\right)^2}{\sum_{1}^{N}\left(\hat{y}_i - \bar{y}_i\right)^2} \quad \text{Eq.14}$$

$$IME = \frac{1}{b-a}\int_a^b (\hat{y}_i - y_i) d\, log|h| \quad \text{Eq.15}$$

$$IRMSE = \left[\frac{1}{b-a}\int_a^b (\hat{y}_i - y_i)^2 d \log|h|\right]^{1/2} \quad \text{Eq.16}$$

$$RI = \frac{IRMSE_1 - IRMSE_i}{IRMSE_1} \times 100 \quad \text{Eq.17}$$

٢٥١

٢٥٢ where n_p is the number of estimated factors in the model; N is the total number of soil samples
٢٥٣ used to estimate K, y_i, $\hat{y}_i$ and $\bar{y}_i$ are observed, estimated, and average of the observed values of K,
٢٥٤ respectively; and h is the matric suction (kPa). IRMSE can only have positive values. The
٢٥٥ estimation accuracy increases as the IRMSE values tend toward zero (Tietje and Tapkenhinrichs,
٢٥٦ 1993). In the RI criterion, $IRMSE_1$ is the IRMSE of PTF_1 and $IRMSE_i$ is the IRMSE of $PTF_{2\text{-}16}$.
٢٥٧ In general, the lower the AIC and IRMSE, the better the model (Whiting et al., 2004). R^2 is the
٢٥٨ proportion of variation in the outcome that is explained by the estimator variables, and the higher
٢٥٩ the R^2, the better the model (Kassambara, 2018). The higher the RI, the more accurate the models.
٢٦٠ The IME results show positive and negative differences between the estimated and observed
٢٦١ values. A positive IME (IME>0) indicates an underestimation, whereas a negative IME value
٢٦٢ (IME<0) indicates an overestimation compared with the observed values (Tietje and
٢٦٣ Tapkenhinrichs, 1993).

3. Results and discussion

3.1. Description of the training and testing steps

Table 4 summarizes the statistics of all variables for the training and testing steps.

Table 4. Summarizes all factors' statistical data.

Factors [a]	Max	Min	Standard deviation (SD)	Mean	Max	Min	Standard deviation (SD)	Mean	p-value of t-test
	Training (53)				Testing (52)				
Si/Sa	6.06	0.24	107.64	1.66	5.48	0.17	106.01	1.49	0.99
C	29.71	4.11	676.08	12.83	52.60	4.89	1133.18	15.69	0.60
BD	1.87	1.15	16.16	1.46	1.78	1.13	15.62	1.43	0.441
CEC	53.58	6.20	1176.01	24.96	40.77	1.08	1165.05	22.12	0.60
Θ_{sv}	66.69	31.45	848.91	48.27	70.70	32.45	872.90	49.54	0.52
PR	8009	687	144830	2530	11305	532	161275	2167	0.52
TS	15.23	5.88	290.19	9.35	22.35	5.35	340.46	10.11	0.66
P_c	630	71	12796	251	630	63	14068	266	0.83
C_c	0.88	0.25	11.66	0.54	0.79	0.16	14.03	0.53	0.88
C_s	0.03	0.00	0.54	0.01	0.04	0.00	0.59	0.01	0.66
a	0.64	0.00	12.69	0.13	1.05	0.00	20.03	0.15	0.50
b	2.97	1.30	38.61	2.16	3.45	0.79	48.45	2.01	0.25
c	1.44	0.35	22.72	0.72	1.42	0.30	20.35	0.71	0.89
m	3.64	2.61	23.22	3.06	4.24	2.39	33.94	3.09	0.68
α	1.20	0.03	17.08	0.15	0.50	0.03	9.61	0.15	0.59
K_0	42.96	0.01	748.96	2.46	16.90	0.02	295.31	1.65	0.745
α^*	0.007	0.000	0.141	0.004	0.049	0.002	0.634	0.005	0.10
n^*	5.02	1.34	54.56	1.97	2.72	1.24	35.55	1.85	0.77
e_0	1.69	0.40	23.91	0.81	2.00	0.47	27.07	0.86	0.39
σ_i	11962	1915	196474	4338	15927	1893	219086	4049	0.22
σ_{mc}	3679	944	50831	1726	3433	500	56283	1561	0.17

a. Table 2 provides an explanation of these factors.

The values of soil texture and structure factors have a wide range. These ranges are 0.17-6.06 for the Si/Sa, and 4.11-52.60 % for clay. Four regions of Iran were used to collect soil samples with various vegetation type, including forests, dry lands, and barren land. Soil samples from East Azarbaijan with 0.39 % OM content and sandy loamy textures had the

highest BD. The high BD is due to low OM content or local compaction. The soil samples from Hamedan with 0.58% OM content had the lowest BD.

Despite the low OM content, the low BD may be due to the fact that the samples were collected from a forest region where grazing was limited, which has a positive influence on soil conservation management (especially against livestock) (Barrio, 2007).

P_c values were highest and lowest in the samples from Kermanshah and Hamedan provinces with 1.27 % and 0.27% OM content, respectively, and both samples had a silty loam texture. This result shows the effect of factors other than soil texture, such as soil structure and OM content, on pre-compression stress. The SD (Table 4) for most soil characteristics is large, indicating moderate to high soil characteristics variability, which is common for soils (Mulla and McBratney, 2002). Physical characteristics are spatially variable over a range of distances; thus, it is necessary to improve the accuracy of determining the spatial variability of physical characteristics (Mitchell-Fostyk, 2021).

The p-values of the t-test results are reported in Table 4. There was no significant difference between the two data sets (testing and training) for any of the variables. The USDA texture triangle of the 105 soil samples shows that most samples have medium- to fine-textured soils (Fig. 3).

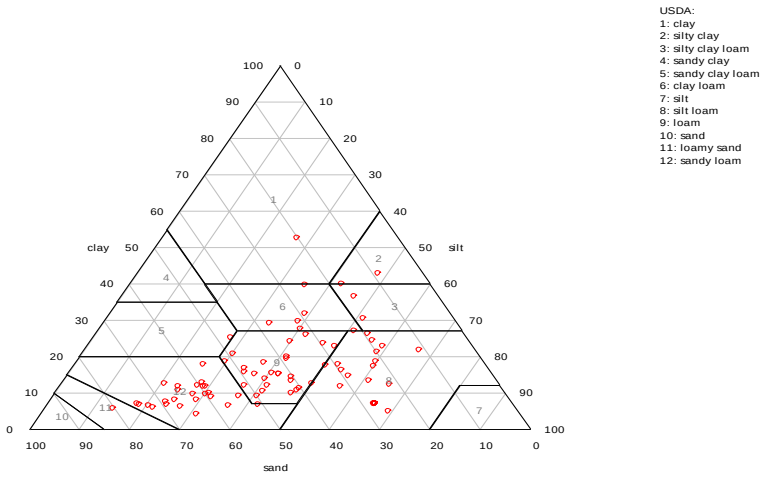

Fig. 3. USDA texture triangle.

3.2. Correlation between the factors

For the training and testing steps (Table 5), the factors used in the PTFs were compared using the Pearson correlation coefficient. Basic soil characteristics and physical-mechanical soil characteristics were typically found to have strong and significant correlations. The correlation between soil characteristics is, in turn, essential for creating PTFs.

Table 5. Correlation between physical and mechanical soil characteristics

	Si/Sa	C	BD	CEC	θ_{sv}	PR	TS	α	K_0
Si/Sa[a]	1								
C	0.20*	1							
BD	-0.21*	-0.29**	1						
CEC	0.37**	0.30**	-0.40**	1					
θ_{sv}	0.41**	0.46**	-0.70**	0.48**	1				
PR	0.01	-0.11	0.63**	-0.22*	-0.50**	1			
TS	-0.01	0.39**	-0.16	0.08	0.47**	-0.22*	1		
α	0.14	0.17	-0.11	0.03	0.14	0.02	0.09	1	
K_0	0.23*	0.22*	0.07	-0.05	0.06	0.27**	0.10	0.82**	1
Pc	0.22*	0.32**	0.16	0.08	0.30**	0.02	0.44**	0.19	0.24*
Cc	0.01	0.10	-0.45**	0.22	0.10	-0.29**	-0.22*	-0.21*	-0.30**
Cs	-0.18	0.06	-0.45**	0.09	0.10	-0.21*	-0.07	0.16	-0.06
a	0.08	0.07	-0.45**	0.17	0.28**	-0.27**	-0.11	0.19	0.07
b	0.34**	-0.01	0.11	0.11	0.03	0.16	-0.30**	-0.15	-0.03
c	-0.25*	0.19*	-0.59**	0.15	0.24*	-.45**	0.18	-0.02	-0.21*
m	0.09	0.08	0.34**	-0.04	0.0003	0.19*	0.34**	0.01	0.06
α*	-0.07	0.09	-0.16	-0.09	0.08	-0.09	0.17	0.05	0.01
n*	0.12	-0.23*	0.21*	-0.26*	-0.28**	0.18	-0.41**	-0.20*	-0.06
σ_i	0.43**	0.32**	0.06	0.24*	0.31**	0.05	0.25*	0.12	0.20*

σ_{mc}	0.42**	0.19	0.24*	0.13	0.11	0.24*	0.02	-0.10	0.08
e_0	-0.12	0.19	-0.68**	0.24*	0.26**	-0.43**	0.01	0.07	-0.14

* and ** show significant correlations at $p < 0.05$ and $p < 0.01$, respectively.
[a]. Abbreviations are listed in Table 2.

The Si/Sa ratio shows a positive and significant correlation (at the confidence interval of 5%), with K_0 (factor of the Gardner model) (Table 5). Gülser et al. (2016) reported that K_0 significantly increased with increasing Sa and Si content. Wang et al. (2012) reported a positive and significant correlation between clay and hydraulic conductivity ($P<0.05$). The soils used in the current study were sampled from various locations, with most samples being from agricultural areas with controlled and conservation tillage, showing a texture class from medium to fine. Therefore, suitable soil management (Barrio, 2007) may have resulted in an increase in soil pores and better aeration of the soil, resulting in a relative decrease in BD (Castellini et al., 2020) and an increase in K_0. The PR ($P<0.01$), P_c ($P<0.01$) and σ_i ($P<0.05$) factor had a positive and significant correlation with K_0 (Table 5). Furthermore, the c and C_c ($P<0.05$) factor had a negative and significant correlation with the Gardener's K_0 factor (Table 5). The correlation of hydraulic conductivity with soil structure and factors such as Pc, Cc, and Cs can reveal their impact on hydraulic conductivity (Gubiani et al., 2015). Argote-Sanchez et al. (2019) found a strong correlation between soil hydraulic function and soil characteristics. An increase in the compression index indicates a decrease in resistance against applied forces, whereas a lower resistance indicates a weaker structure, causing damage and a decrease in K. This suggests a negative correlation between compression and K0. At lower suctions, pore water tolerates most outside pressure without affecting the soil structure. At zero suction, water leaves pores; however, at higher suctions, pressure destroys large pores, leaving small ones, resulting in a decrease in K (Zeng and Shao, 2022). The correlation between the mechanical and hydraulic factors indicates a physical connection between these two groups. Studying this correlation facilitates the understanding of the

relationship between soil characteristics and increase the accuracy and reliability of PTFs (Bayat et al., 2011).

3.3. Parametric transfer functions of K with Gardner model (1985)

Some researchers have also reported that the regression result is better than the neural network (Duliba, 1991; Gorr et al., 1994). In addition, researchers such as D'Emilio et al. (2018) and Ghanbarian et al. (2015) reported that the ANN method is more appropriate for estimating hydraulic characteristics than regression. Heiat (2002) and Minasny et al. (1999) also found that the ANN method is as effective as the nonlinear regression method. SubbaNarasimha et al. (2000) found that ANNs have poor estimations. To determine the situations in which ANNs provide a more accurate estimate, systematic empirical studies are needed, using data sets based on variable number, noise, and sample size.

In this research, according to the results in Table 6, the results of the neural network method are weak compared with those of the regression method. Therefore, the regression method's findings were examined in order to shorten the text.

Table 6. Results of the estimation of by the MLR and ANN methods

PTFs	IME[b] (cmh^{-1})	IRMSE (cm/h)	R^2	AIC	RI	IME (cmh^{-1})	IRMSE (cmh^{-1})	R^2	AIC	RI
	Train (MLR)					Train (ANN)				
PTF_1[a]	-0.475	1.145	0.956	949		-0.36	0.89	0.96	1072	
PTF_2	-0.431	1.018	0.959	855*	11.12	-0.38	0.92	0.96	1074	-3.39
PTF_3	-0.437	1.022	0.958	856*	10.72	-0.36	0.94	0.96	1053	-5.25
PTF_4	-0.446	1.115	0.962	884*	2.63	-0.27	0.87	0.64	926*	2.13
PTF_5	-0.307	0.777	0.957	401*	32.13	-0.27	0.69	0.96	279*	22.22
PTF_6	-0.310	0.767	0.955	396*	32.99	-0.26	0.65	0.96	90*	26.84
PTF_7	-0.307	0.730	0.956	392*	36.20	-0.36	0.88	0.96	935*	1.51
PTF_8	-0.413	1.049	0.959	841*	8.37	-0.35	0.99	0.77	1146	-11.66
PTF_9	-0.437	1.128	0.958	873*	1.50	-0.41	1.05	0.73	1237	-18.22
PTF_{10}	-0.294	0.743	0.959	377*	35.05	-0.35	0.88	1.00	991*	0.95
PTF_{11}	-0.376	1.035	0.945	436*	9.55	-0.53	1.25	0.96	1415	-40.12

PTFs	IME[b] (cmh^{-1})	IRMSE (cm/h)	R^2	AIC	RI	IME (cmh^{-1})	IRMSE (cmh^{-1})	R^2	AIC	RI
PTF_{12}	-0.441	1.118	0.957	943	2.30	-0.37	0.93	0.96	1091	-4.47
PTF_{13}	-0.475	1.090	0.954	929	4.75	-0.38	0.92	0.96	1074	-3.34
PTF_{14}	-0.385	0.941	0.958	703*	17.80	-0.34	0.90	0.96	1011*	-0.57
PTF_{15}	-0.355	0.807	0.948	445*	29.53	-0.31	0.72	0.97	397*	19.46
PTF_{16}	-0.477	1.116	0.960	837*	2.52	-0.38	0.94	0.94	1117	-4.99
		Test (MLR)					Test (ANN)			
PTF_1	-0.333	1.031	0.953	464		-0.40	0.89	0.97	151	
PTF_2	-0.116	0.738	0.952	-240*	28.48	-0.50	1.06	0.97	176	-19.15
PTF_3	-0.094	0.764	0.955	-201*	25.90	-0.47	1.12	0.97	164	-25.25
PTF_4	-0.088	0.883	0.947	85*	14.34	-0.38	0.93	0.69	106*	-4.85
PTF_5	-0.241	0.683	0.958	-159*	33.75	-0.48	1.14	0.97	179	-28.32
PTF_6	-0.249	0.693	0.960	-142*	32.80	-0.50	1.11	0.97	178	-24.50
PTF_7	-0.256	0.752	0.958	-59*	27.05	-0.45	1.17	0.97	173	-31.57
PTF_8	0.235	1.405	0.951	869	-36.19	-0.50	1.16	0.78	196	-30.34
PTF_9	-0.103	0.723	0.942	-245*	29.93	-0.29	0.77	0.77	70*	13.32
PTF_{10}	-0.175	0.749	0.949	-150*	27.33	-0.33	1.07	1.00	135*	-19.95
PTF_{11}	-0.346	0.863	0.964	36*	16.36	-0.44	1.03	0.97	124*	-15.48
PTF_{12}	-0.117	0.886	0.954	-0.73*	14.05	-0.50	1.04	0.97	163	-17.30
PTF_{13}	-0.262	0.742	0.960	-91*	28.00	-0.50	1.06	0.97	176	-19.22
PTF_{14}	0.204	1.283	0.955	775	-24.42	-0.44	1.18	0.97	175	-32.07
PTF_{15}	-0.338	0.747	0.960	-40*	27.59	-0.56	1.07	0.97	183	-20.44
PTF_{16}	-0.168	0.868	0.948	159*	15.88	-0.46	1.03	0.96	122*	-15.65

٣٤٤ * Indicates a significant improvement ($p < 0.05$) based on the AIC criterion.

٣٤٥ [a.] Table 3 shows the input factors of the PTFs.

٣٤٦

٣٤٧

٣٤٨

٣٤٩ ***First Group***

٣٥٠ Basic soil characteristics were used to determine K at this level. (Table 6). Various researchers,

٣٥١ such as Vereecken et al. (1990), have used these factors to estimate K using the regression method.

٣٥٢ Gamie and De Smedt (2018) estimated K using basic soil characteristics such as silt and clay, field

٣٥٣ capacity moisture, and other basic soil characteristics. Zhang et al. (2019) evaluated K using basic

٣٥٤ soil characteristics and reported the best state-space model, which comprised silt, clay, and

٣٥٥ macroporosity, and acceptable performance ($R^2 > 95\%$) in characterizing the spatial variability of

٣٥٦ K. Bayat et al. (2015) estimated K using the van Genuchten–Mualem model by creating parametric

٣٥٧ transfer functions and using the basic soil characteristicsused in this study. They reported IRMSE

(cm h^{-1}), R^2, and AIC values of 0.24, 0.98, and 1091, respectively, for the training step and 0.189, 0.970, and 494, respectively, for the testing step.

Second Group

In this group, three PTFs were used. The factors of the CC curve (Pc, Cc, Cs, σi and σmc) along with the basic soil characteristics were applied in this group (Table 3). In all three PTFs, IRMSE and AIC decreased compared with the first group in both training and testing steps, whereas R^2 increased. This means that the factors in this group have a considerable effect on improving the estimation of K (Table 6). Table 5 shows that the Pc factor has a positive and significant correlation (at the significant levels of 5% and 1%) with soil texture (clay and Si/Sa), whereas the Cc and Cs factors showed a negative and significant correlation with BD.

According to An et al. (2015), pre-compression stress has a negative relationship with water content because higher water contents result in more water in the pores and a thicker water film surrounding soil particles. As a result, there is less effective tension and the water-menisci forces between the particles are weaker. The degree of continuity between particles also diminishes as water menisci do (Imhoff et al., 2004). Therefore, K decreases with decreasing pore continuity (Zhai and Horn, 2018). According to Gao et al. (2021), soil moisture is dependent on both soil suction and soil void ratio. To improve the accuracy of K estimation, the characteristics that affect the void ratio can be used as estimators. Baumgartl and Kock (2004) reported that factors in CC curves are dependent on soil structure since hydraulic conductivity reaches its maximum value in rough soils. According to the results of Baumgartl and Kock (2004) and the positive and significant correlation between P_c with soil texture and Gardener's K_0 factors (Table 5), using these factors in PTF_2 improves the accuracy of K estimation. Jariya et al. (2009) observed that P_c and C_c affect

soil structure and that this effect is correlated to the mineral type of clay soil. Therefore, using the factors of the CC curve as an estimator in PTF_4 can be effective for improving K estimations.

In this group, all input factors included the CC curve factors, resulting in a positive RI value at all three levels. This indicates that the inputs have been successful in estimating K at all three levels. However, PTF_2 has better results in this group, probably because of its large number of inputs.

Third Group

In this group, four PTFs were used. The factors of the CC curve (α^* and n^* factors of the $VG_{modified}$ model, e_0, Gompertz model coefficient) along with the basic soil characteristics were applied in this group (Table 3). The results indicated that in all four PTF_s in this group, IRMSE and AIC decreased compared with the first group in both training and testing steps, whereas R^2 increased, indicating a significant effect of input factors on the estimation of K (Table 6). In PTF_5, the similarity in the shape of the CC and K curves improved the accuracy and reliability of the K estimations. Gregory et al. (2006) stated that the Gompertz model coefficient is equivalent to the CC curve factors. For example, the coefficient "a" of the Gompertz model is equivalent to e_0. Therefore, using the Gompertz model coefficient improved the accuracy and reliability of the K estimations in PTF_7. According to the results presented in Table 6, the results of PTF_8 are weaker than those of PTF_7, so PTF_8 not only shows significant changes during the testing step but also fails to improve the estimation results. The reason for this result is probably the negative and high correlation of the Gampertz model coefficients with BD (Table 5).

In this group, the best results were observed for PTF_6, which used α^*, n^*, and e_0 factors along with basic soil characteristics. The n^* factor is the slope of the soil moisture retention curve and determines the distribution of pores in the suction range (Van Genuchten, 1980). In the van Genuchten model, all factors are correlated to the particle size distribution, either directly or

indirectly. Therefore, with an increase in the number of small pores, the water retention of the soil under saturated conditions increases. The reason for increased water retention in the soil can be related to the increase in overall soil porosity with an increase in small pores (Van Genuchten, 1980).

This study used tension disc infiltration to measure K in agricultural soils with soil management and protective tillage. Conservation tillage improves soil structure, particle stability, and physical quality, leading to increased large pores and higher e_0 (Dalla Rosa et al., 2012; da Silva et al., 2012). As can be seen in the correlation table (Table 5), e_0 and BD have a negative and significant correlation, whereas the van-Genuchten α^* factor has no significant correlation with BD. Conservation tillage and soil management, increase the porosity of protected areas with a decrease in BD (Johnson et al., 2016). Consequently, a decrease in BD, increases the e0 factor, leading to significant effects on the estimation of K. This is probably because this level performed better than the other levels.

Fourth Group

This group includes two PTFs. PTF_9 used TS factors and PTF_{10} used PR factors along with basic soil characteristics as the estimator variables. During both training and testing steps, IRMSE and AIC decreased compared with the first group and R^2 increased, indicating a significant effect of factors in this group on improving the estimation of K (Table 6).

TS is a dynamic soil characteristic that affects fracture strength, air-filled pores, micro-cracks, and bonding strength (Zhu, 2018). It correlates with moisture content, processes, and particle continuity (Abid and Lal, 2009). Using TS as an estimator improves the estimation results. Reis et al. (2013) found that agricultural management systems impact soil TS and friability by increasing OM content and bonding strength. Çelik et al. (2019) reported that tillage can increase the K_0 while

decreasing PR and BD due to decreased compactness because of tillage. According to Table 5, PR shows a positive and significant correlation with the K_0 factor of the Gardner model (1958). This positive correlation results in improved estimation accuracy. Both K (Kumar et al., 1994) and PR (To and Kay, 2005) have high variability. Therefore, PR can show changes in K and is a suitable factor for its estimation. For, this reason, PTF_{10} probably shows the best results among all PTF_s (a total of 16 PTF_s) used in the present study.

Fifth group

This group includes two PTF_s. PTF_{11} function used CEC and PTF_{12} used θ_{sv} along with basic soil characteristics as the estimators. In this group, PTF_{11} inputs increased IRMSE and AIC and increased R^2 compared with the first group in both the training and testing steps. These input factors showed a significant improvement in estimating K. Therefore, this group also relatively improved the estimation of K (Table 6). According to Table 5, CEC has a positive and significant correlation with clay and Si/Sa and a negative and significant correlation with BD. Probably because of these correlations, this factor improved the estimation of K. Moosavi and Sepaskhah (2012) created transfer functions using physical and chemical soil characteristics using the regression method to estimate K using a permeameter at different suction. They reported that the best results were obtained when θ_{sv}, cation exchange capacity to electrical conductivity ratio (CEC/ EC), and the sand content were used to estimate K_0

Sixth group

This group includes four PTF_s, and the input factors for each function are presented in Table 3. Unlike all previous groups, in this group, basic soil characteristics were not used. According to

Table 6, after removing basic soil characteristics from the model's input, the results are weaker in both training and testing steps compared with PTF_s using basic soil characteristics (group 2 and 3 results). Among the PTF_s in this group, the results of PTF_{15}, which used α^*, n^*, and e_0 factors, have the lowest IRMSE and AIC values and were the most reliable. As shown in Table 6, the factors of the CC curve (P_c, C_c, and C_s) had no significant effects on the estimation during the training step. This is probably due to the negative and significant correlation between C_s and C_c factors and BD (Table 5). However, due to the negative and significant correlation of e_0, the coefficients "a" and "c" of the Gompertz model with BD, and the positive and significant correlation between σ_{mc}, and σ_i with the Si/Sa, the K estimation improved at other levels in group 6. The weaker results in group 6 compared with those in groups 2 and 3 when using basic soil characteristics is probably due to the lower number of inputs for each function in group 6.

In the present study, among 6 groups of PTF_s, PTF_{10} in group 4 showed the best results. At this level, PR has been used along with basic soil characteristics as input variables. in this study, most soil samples were taken from agricultural lands with conservation tillage and soil management. Conservation tillage is a system of producing agricultural products while managing and maintaining plant remains where at least 30% of the land is covered in plant remains after harvest (Nyakudya and Stroosnijder, 2015). The OM content increases the stability of the soil structure and soil elasticity, resulting in decreased soil compactness (An et al., 2010). Therefore, tillage results in a decrease in PR and an increase in K. Villarreal et al. (2020) investigated K during the crop cycle using both conventional and no-tillage techniques and found that the conventional technique had higher K and water-conducting macroporosity values. It has been observed that tillage can increase the total macroporosity values over time. Therefore, by increasing the

biological activity during the growth phase, the connection of soil macropores is increased and thus the transport of water in the soil is enhanced.

The IME value is negative in most transfer functions in Gardener's model (IME<0), indicating an overestimation. This means that there is a systematic error in the estimated values compared with the observed values. According to Table 6, the IME values show that the estimated values have a regular error compared with the observed values, and its correction ability is better than irregular error. This result shows the high performance of the model in estimating the results. Table 7 shows the models and regression coefficients for the estimation of the Gardner model factors (K_0 and α).

Table 7. Regression models of the estimation of Gardner model factors (K_0 and α).

PTF	Output	Model and coefficients
PTF_1[a]	α	-0.109×S/S+0.385×C- 0.124×BD - 0.02
	K_0	-0.207×S/S+0.609×C+0.08×BD+0.0001
PTF_2	α	-0.057×S/S+0.382×C-0.242×BD+75×Pc -0.484 ×Cc +0.309 ×Cs +0.003
	K_0	-0.219×S/S+0.535×C-0.156×BD+137×Pc -0.526 ×Cc +0.149 ×Cs +0.02
PTF_3	α	-0. 126× S/S +0.431 ×C - 0.318 ×BD -0.428×Cc -0.003
	K_0	-0. 243× S/S +0.647 ×C - 0.155 ×BD -0.053×Cc -0.023
PTF_4	α	0.146×S/S+0.268×C+0.1×BD+0. 811×σ_i -1.032×σ_{mc} +0.014
	K_0	-0.097×S/S+0.556×C+0.234×BD+0. 577×σ_i -0.712×σ_{mc} +0.067
PTF_5	α	-0.029×S/S+0.341×C-0.071×BD-0.061×α^*+0.062×n^* -0.046
	K_0	-0.299×S/S+0.508×C+0.148×BD-0.01×α^*-0.083×n^* -0.035
PTF_6	α	-0.324×S/S+0.319×C-0.089×BD-0.054×α^*+0.08×n^* -0.013×e_0 -0.06
	K_0	-0.367×S/S+0.505×C+0.033×BD+0.003×α^*-0.086×n^* -0. 153×e_0 -0.043
PTF_7	α	-0.01×S/S+0.442×C-0.249×BD+0.391×a -0.435 ×b -0.492 ×c +0.106×m -0.093
	K_0	-0.256×S/S+0.687×C-0.223×BD+0.269×a -0.386 ×b -0.696 ×c -0.015×m -0.076
PTF_8	α	-0.055×S/S+0.471×C-0.008×BD+0.444×a+0.13×m +0.025
	K_0	-0.379×S/S+0.761×C-0.228×BD+0.235×a-0.540×c +0.042
PTF_9	α	-0. 077× S/S +0.559 ×C - 0.085 ×BD -0.029×TS +0.066
	K_0	-0. 237× S/S +0.541 ×C+ 0.103 ×BD +0.224×TS +0.092
PTF_{10}	α	-0. 147× S/S +0.414 ×C - 0.217 ×BD +0.012×PR -0 .034
	K_0	-0. 191× S/S +0.599 ×C + 0.124 ×BD -0.052×PR+0.003
PTF_{11}	α	-0.037× S/S -0.089 ×C - 0.107 ×BD +0.027×CEC +0.193
	K_0	0.32× S/S -0.104 ×C - 0.017 ×BD -0.158×CEC +0.461
PTF_{12}	α	-0. 126× S/S +0.351 ×C - 0.068 ×BD +0.095×θ_S -0 .027
	K_0	-0. 292× S/S +0.376 ×C + 0.520 ×BD +0.068×θ_S +0.008
PTF_{13}	α	160×Pc -0.285 ×Cc +0.429 ×Cs +0.048
	K_0	263×Pc -0.375 ×Cc +0.303 ×Cs +0.086
PTF_{14}	α	0.036×a -0.501 ×b -0.222 ×c +0.087×m +0.038
	K_0	0.211×a -0.704 ×b -0.049 ×c -0.045×m -0.017
PTF_{15}	α	-0.027×α^*-0.057×n^* +0.152×e_0 -0.118
	K_0	0.056×α^*-0.28×n^* -0.057×e_0 -0.131
PTF_{16}	α	0.0004+0.915×σ_i -1.009×σ_{mc}

K_0	$-0.022+0.867\times\sigma_i -0.865\times\sigma_{mc}$

a. Tables 2 and 3 display the PTF input factors.

A 1:1 curve can be used to evaluate the performance of PTF_s. The low difference between the estimated and observed values and proximity to the 1:1 line indicates the high performance of PTF_s in estimating soilK, whereas a large distance from the 1:1 line indicates the weak performance of PTF_s (Moosavi and Sepaskhah, 2012). To evaluate the validity of PTF_s, the correlation between the observed and estimated K values was calculated. The fitted regression line was compared with the line passing through (x=0, y=0) with a slope of 1:1. The best results are obtained when the difference between the estimated and observed values is minimized. Figure 4 shows the high capability of the created PTF_s for measuring K. The slope of the regression line in the created models for estimating K is close to 1. As a result, it is possible to conclude that the provided models are highly reliable

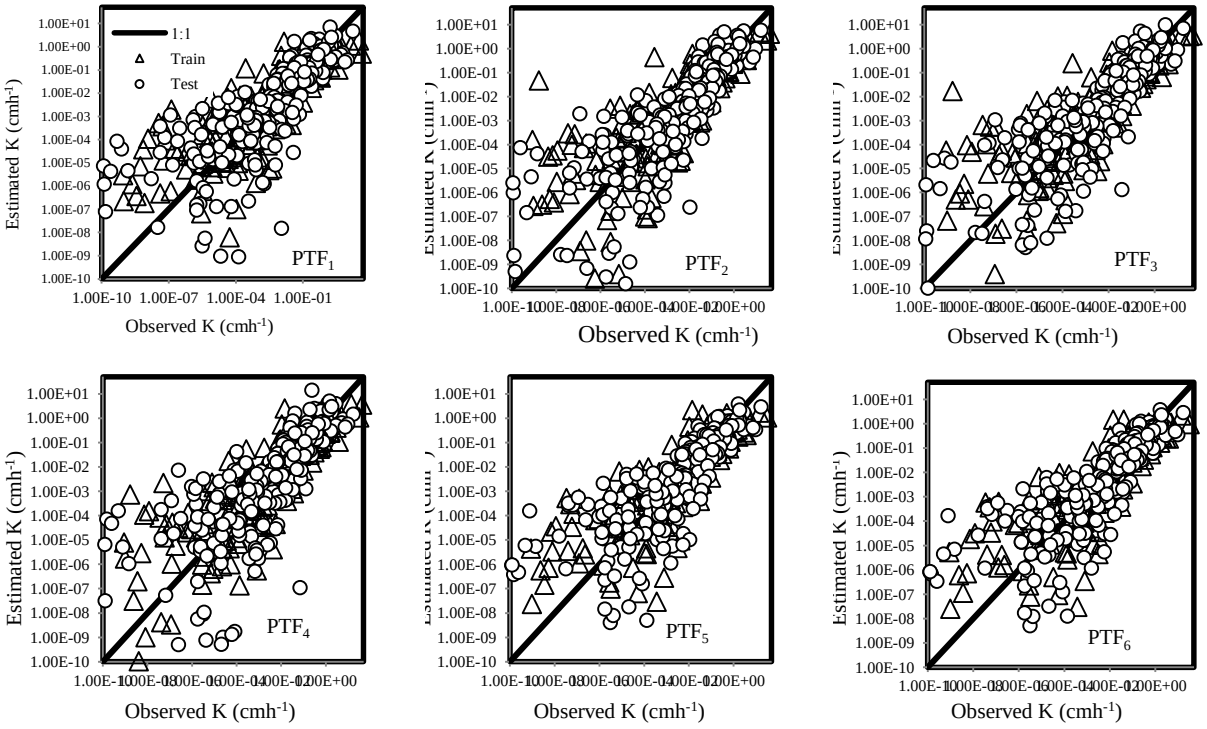

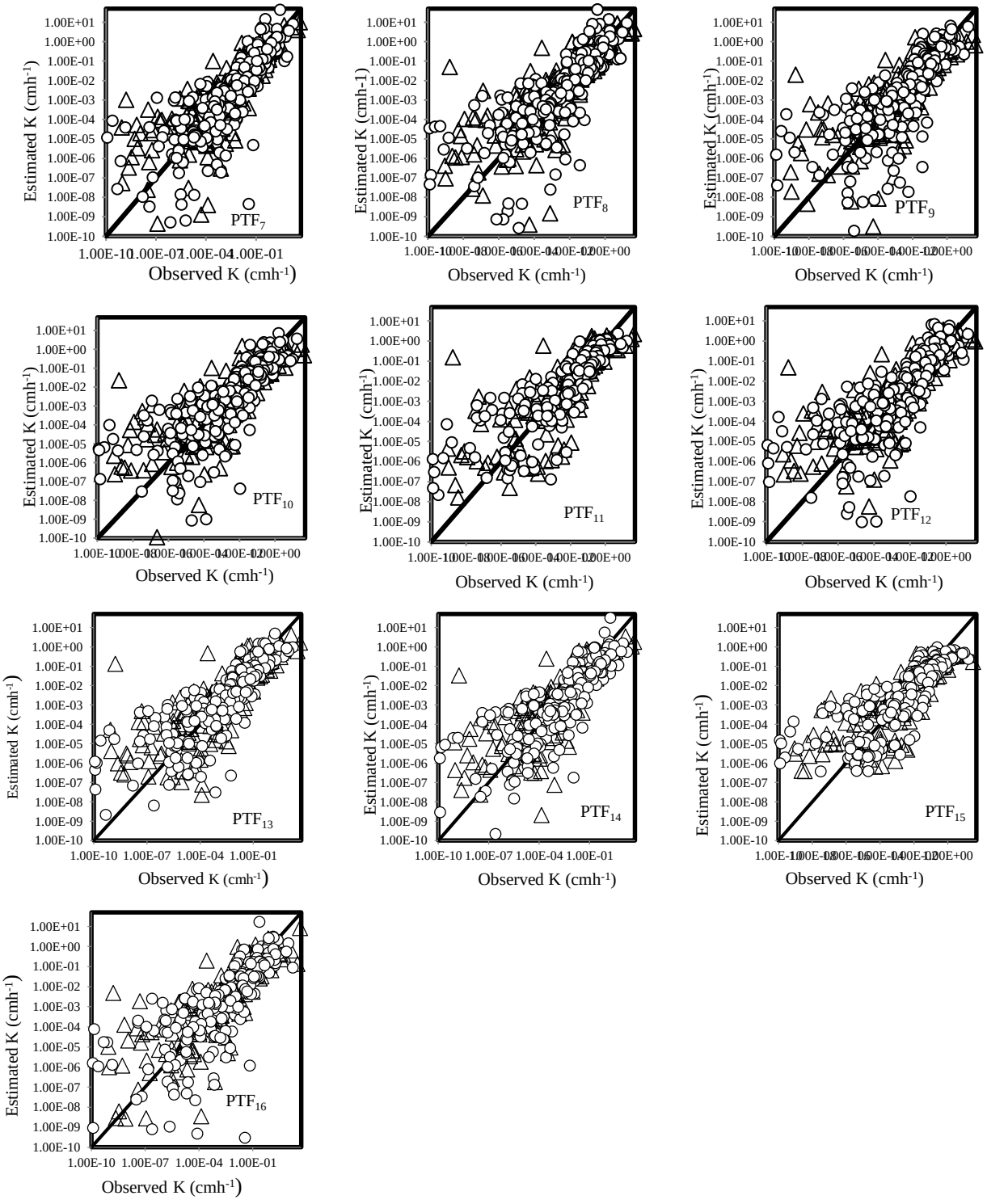

٤٩١ Fig 4. Observed versus estimated values of K using MLR methods.

٤٩٢

٤٩٣

٤٩٤ **4. Conclusion**

Because of soil heterogeneity, it is challenging to assess the hydraulic conductivity of soil on a field scale. To better understand soil hydraulic processes, accurate methods for measuring the soil hydraulic characteristics are required. PTF_s also play an important role in quantifying and estimating the ecosystem services of soils. The development of PTFs to estimate hydraulic factors from soil characteristics is an active area of research. These studies often incorporate advanced multivariate statistical techniques to build their estimation models. According to the results, the following conclusions can be reported:

1. PTF_{10}, which used PR along with the basic soil characteristics, has the best relative results. This may be due to the positive effects of conservation tillage and soil management of the agricultural fields, resulting in an increase in OM content. This, in turn, results in higher stability of soil particles and lower PR, leading to improved estimation of K when used as input for the model.

2. The estimation of K was improved in both the training and testing steps by all inputs, except for PTF_7 and TTF_{14}. Therefore, no overestimation has occurred in this study, and the regression has full coverage for both training and testing steps. The error decreases by presenting the new data to the model as input, indicating a suitable reaction toward the new data. Therefore, it can be concluded that these models have reached a suitable generalization.

3. According to the results, it can be concluded that the results in groups 2, 3, and 6, which used factors from the CC curve as input in the models, have resulted in significant improvement in the estimation of K. Therefore, it can be concluded that because of the relative appearance similarity between the CC curve and K curve, they are affected by similar factors such as OM content, e_0, and the number of large pores. These soil

characteristics affect both curves, resulting in an improvement in the estimation of K using the CC curve factors, with or without basic soil characteristics.

4. Finally, it can be suggested that soil management and improvement to prevent soil compaction can be used to manage water movement in agricultural soils and improve production yields.

Authorship contribution statement

Azadeh Sedaghat (project administration, investigation, software, visualization, investigation, and writing—original draft preparation and editing); Hossein Bayat (supervision), Seyed Majid Mousavi (investigation, and writing—original draft preparation and editing).

Data availability

The datasets generated during and/or analysed during the current study are not publicly available due to personal reasons but are available from the corresponding author on reasonable request.

Conflicts of interest

The author(s) declare(s) that there is no conflict of interest regarding the publication of this article.

Funding statement

The authors declare that no funds, grants, or other support were received during the preparation of this manuscript.

References

Abid, M., Lal, R., 2009. Tillage and drainage impact on soil quality: II. Tensile strength of aggregates, moisture retention and water infiltration. Soil and Tillage Research, 103(2), 364-372 .

Adab, H., Morbidelli, R., Saltalippi, C., Moradian, M ,. Ghalhari, G. A. F., 2020. Machine learning to estimate surface soil moisture from remote sensing data. Water, 12(11), 3223 .

Agyare, W. A., Park, S., Vlek, P., 2007. Artificial neural network estimation of saturated hydraulic conductivity. Vadose Zone Journal, 6(2), 423-431 .

Akaike, H., 1974. A new look at the statistical model identification. IEEE transactions on automatic control, 19(6), 716-723.

Al-Jabery, K., Obafemi-Ajayi, T., Olbricht, G., Wunsch, D. 2019. Computational Learning Approaches to Data Analytics in Biomedical Applications: Academic Press.

Ali, A. R., 2018. Vertical Hydraulic Conductivity of Unsaturated Zone by Infiltrometer Analysis of Shallow Groundwater Regime (KUISG). Journal of University of Babylon for Engineering Sciences, 26(4), 185-194 .

Amini, M., Abbaspour, K. C., Khademi, H., Fathianpour, N., Afyuni, M., Schulin, R., 2005. Neural network models to predict cation exchange capacity in arid regions of Iran. European Journal of Soil Science, 56(4), 551-559 .

An, J ,.Zhang, Y., Yu, N., 2015. Quantifying the effect of soil physical characteristics on the compressive characteristics of two arable soils using uniaxial compression tests. Soil and Tillage Research, 145, 216-223 .

An, S., Mentler, A., Mayer, H., Blum, W .E., 2010. Soil aggregation, aggregate stability, organic carbon and nitrogen in different soil aggregate fractions under forest and shrub vegetation on the Loess Plateau, China. CATENA, 81(3), 226-233 .

Angulo-Jaramillo, R., Vandervaere, J.-P., Roulier ,S., Thony, J.-L., Gaudet, J.-P., Vauclin, M.,, 2000. Field measurement of soil surface hydraulic characteristics by disc and ring infiltrometers: A review and recent developments. Soil and Tillage Research, 55(1-2), 1-29 .

Argote-Sanchez, C. L., Lozano-Santa ,J. M., Reyes-Trujillo, A., 2019. Determination of the water regulation capacity of a typic hapludands by means of humidity retention curves and the modeling of its hydrophysical characteristics. Ingeniería y competitividad, 21(1), 103-116 .

Azadmard, B., Mosaddeghi, M. R., Ayoubi, S., Chavoshi, E., Raoof, M. 2020. Estimation of near-saturated soil hydraulic characteristics using hybrid genetic algorithm-artificial neural network. Ecohydrology and Hydrobiology, 20(3), 437-449 .

Barrio, A., 2007. Effects of cattle grazing on woodland soil health at Hatfield. MSc thesis, School of Applied Sciences of Cranfield University ,

Báťková, K., Miháliková, M., Matula, S., 2020. Hydraulic characteristics of a cultivated soil in temperate continental climate determined by mini disk infiltrometer. Water, 12(3), 843 .

Baumgartl, T., Köck, B., 2004. Modeling volume change and mechanical characteristics with hydraulic models. Soil Science Society of America Journal, 68(1), 57-65 .

Bayat, H., Neyshabouri, M., Mohammadi, K., Nariman-Zadeh, N., 2011. Estimating water retention with pedotransfer functions using multi-objective group method of data handling and ANNs. Pedosphere, 21(1), 107-114 .

Bayat, H., Sedaghat, A., Sinegani, A. A. S., Gregory, A. S., 2015. Investigating the relationship between unsaturated hydraulic conductivity curve and confined compression curve. Journal of Hydrology, 522, 353-368 .

Casagrande, A., 1936. The determination of pre-consolidation load and it's practical significance. Paper presented at the Proc. Int. Conf. Soil Mech. Found. Eng. Cambridge, Mass., 1936.

Castellini, M., Stellacci, A. M., Mastrangelo, M., Caputo, F., Manici, L. M., 2020. Estimating the soil hydraulic functions of some olive orchards: Soil management implications for water saving in soils of Salento peninsula (southern Italy). Agronomy, 10(2), 177 .

Çelik, İ., Günal, H., Acar, M., Acir, N., Barut, Z. B., Budak, M., 2019. Strategic tillage may sustain the benefits of long-term no-till in a Vertisol under Mediterranean climate. Soil and Tillage Research, 185, 17-28 .

D'Emilio, A., Aiello, R., Consoli, S., Vanella, D., Iovino, M., 2018. Artificial neural networks for predicting the water retention curve of sicilian agricultural soils. Water, 10(10), 1431 . .

da Silva, L. V., Queiroz ,S., da Silva, M. Q., da Costa, J. M., Fernandes, R., 2012. Use of physical protector in tillage for recovery of degraded areas. Bioscience Journal, 28(3), 366-372 .

Dalla Rosa, J., Cooper, M., Darboux, F., Medeiros, J. C., 2012. Soil roughness evolution in different tillage systems under simulated rainfall using a semivariogram-based index. Soil and Tillage Research, 124, 226-232 .

Dexter, A., Kroesbergen, B., 1985. Methodology for determination of tensile strength of soil aggregates. Journal of Agricultural Engineering Research, 31(2), 139-147 .

Dragonetti, G., Farzamian, M., Coppola, A., Basile, A., Monteiro Santos, F., 2022. In-situ estimation of soil hydraulic and hydrodispersive characteristics by inversion of Electromagnetic Induction measurements and soil hydrological modeling. Hydrology and Earth System Sciences Discussions, 1-38 .

Duliba, K. A., 1991. Contrasting neural nets with regression in predicting performance in the transportation industry. Paper presented at the Proceedings of the Twenty-Fourth Annual Hawaii International Conference on System Sciences.

Gamie, R., De Smedt, F., 2018. Experimental and statistical study of saturated hydraulic conductivity and relations with other soil characteristics of a desert soil. European Journal of Soil Science, 69(2), 256-264 .

Gao, Y., Li, Z., Sun, D .a., Yu, H., 2021. A simple method for predicting the hydraulic characteristics of unsaturated soils with different void ratios. Soil and Tillage Research, 209, 104913 .

Gardner, W., 1958. Some steady-state solutions of the unsaturated moisture flow equation with application to evaporation from a water table. Soil science, 85(4), 228-232 .

Castellini, M., Stellacci, A.M., Barca, E., Iovino, M.2019. Application of multivariate analysis techniques for selecting soil physical quality indicators: A case study in long-term field experiments in Apulia (southern Italy). Soil Sci. Soc. Am. J, 83, 707–720.

Gee, G. W., Or, D., 2002. 2.4 Particle-size analysis. Methods of soil analysis. Part, 4(598), 255-293 .

Ghanbarian, B., Taslimitehrani, V., Dong, G., Pachepsky, Y .A., 2015. Sample dimensions effect on prediction of soil water retention curve and saturated hydraulic conductivity. Journal of Hydrology, 528, 127-137 .

Gompertz, B., 1825. XXIV. On the nature of the function expressive of the law of human mortality ,and on a new mode of determining the value of life contingencies. In a letter to Francis Baily, Esq. FRS andc. Philosophical transactions of the Royal Society of London(115), 513-583 .

Gorr, W. L., Nagin, D., Szczypula, J., 1994. Comparative study of artificial neural network and statistical models for predicting student grade point averages. International Journal of Forecasting, 10(1), 17-34 .

Gregory, A., Whalley, W., Watts, C., Bird, N., Hallett, P., Whitmore, A., 2006. Calculation of the compression index and precompression stress from soil compression test data. Soil and Tillage Research, 89(1), 45-57 .

Grossman, R., Reinsch, T., 2002. 2.1 Bulk density and linear extensibility. Methods of soil analysis: Part 4 physical methods, 5, 201-228 .

Gubiani, P. I., Jong Van Lier, Q. d., Reichert, J. M., Goulart, R. Z., Fontanela, E., 2015. Precompression stress and compression index depend on the property used to represent the soil deformation in the compression curve. Ciência Rural, 46, 76-82 .

Gülser, C., Ekberli, I., Candemir, F., 2016. Spatial variability of soil physical characteristics in a cultivated field. Eurasian Journal of Soil Science, 5(3), 192-200 .

Gunarathna, M., Sakai, K., Nakandakari, T., Momii, K., Kumari, M., Amarasekara, M. G. T. S., 2019. Pedotransfer functions to estimate hydraulic characteristics of tropical Sri Lankan soils. 190, 109-119 .

Heiat, A., 2002. Comparison of artificial neural network and regression models for estimating software development effort. Information and software Technology, 44(15), 911-922 .

Ho, R., 2006. Handbook of univariate and multivariate data analysis and interpretation with SPSS: Chapman and Hall/CRC.

Johnson, J. M., Strock, J. S., Tallaksen, J. E., Reese, M., 2016. Corn stover harvest changes soil hydrology and soil aggregation. Soil and Tillage Research, 161, 106-115 .

Kassambara, A., 2018. Machine learning essentials: Practical guide in R: Sthda.

Keller, T., Lamandé, M., Schjønning, P., Dexter, A. R., 2011. Analysis of soil compression curves from uniaxial confined compression tests. Geoderma, 163(1-2), 13-23.

Kreiselmeier, J., Chandrasekhar, P., Weninger, T., Schwen, A., Julich, S., Feger, K.H., Schwärzel, K. 2020. Temporal variations of the hydraulic conductivity characteristic under conventional and conservation tillage. Geoderma, 362, 114127.

Koolen, A., Kuipers, H., 1989. Soil deformation under compressive forces. In Mechanics and related processes in structured agricultural soils (pp. 37-52): Springer.

Kumar, S., Gupta, S., Ram, S., 1994. Inverse techniques for estimating transmissivity and drainable pore space utilizing data from subsurface drainage experiments. Agricultural Water Management, 26(1-2), 41-58 .

Li, Y.-B., Liu, Y., Nie, W.-B., Ma, X.Y., 2018. Inverse modeling of soil hydraulic parameters based on a hybrid of vector-evaluated genetic algorithm and particle swarm optimization. Water, 10(1), 84 .

Lin, H., Zhang, W., Yu, H., 2014. Hydropedology: linking dynamic soil characteristics with soil survey data. In Application of Soil Physics in Environmental Analyses (pp. 23-50): Springer.

Liu, Y., Qian, J., Yue, H., 2020. Combined Sentinel-1A with Sentinel-2A to estimate soil moisture in farmland. IEEE Journal of Selected Topics in Applied Earth Observations and Remote Sensing, 14, 1292-1310 .

Marquaridt, D. W., 1970. Generalized inverses, ridge regression, biased linear estimation, and nonlinear estimation. Technometrics, 12(3), 591-612 .

Minasny, B., McBratney, A. B., Bristow, K. L., 1999. Comparison of different approaches to the development of pedotransfer functions for water-retention curves. Geoderma, 93(3-4), 225-253 .

Mishra, A., Kumar, B., Dutta, J., 2016. Prediction of Hydraulic Conductivity of Soil Bentonite Mixture Using Hybrid-ANN Approach. Journal of Environmental Informatics, 27(2).

Mitchell-Fostyk, B., 2021. Effects of Slope and Land Management on Soil Hydraulic and Thermal characteristics. University Honors College Middle Tennessee State University ,

Moosavi, A. A., Sepaskhah, A. R., 2012. Pedotransfer functions for prediction of near saturated hydraulic conductivity at different applied tensions in medium texture soils of a semi-arid region. Plant Knowledge Journal, 1(1), 1-9 .

Moustafa, M. M., 2000. A geostatistical approach to optimize the determination of saturated hydraulic conductivity for large-scale subsurface drainage design in Egypt. Agricultural Water Management, 42(3), 291-312 .

Nyakudya, I. W., Stroosnijder, L., 2015. Conservation tillage of rainfed maize in semi-arid Zimbabwe: A review. Soil and Tillage Research, 145, 184-197 .

Patil, N. G., Singh, S. K., 2016. Pedotransfer functions for estimating soil hydraulic characteristics: A review. Pedosphere, 26(4), 417-430 .

Perroux, K., White, I., 1988. Designs for disc permeameters. Soil Science Society of America Journal, 52(5), 1205-1215 .

Picton, p., 2000. Neural Networks. Palgrave, New York .

Ross, P., Smettem, K., 2000. A simple treatment of physical nonequilibrium water flow in soils. Soil Science Society of America Journal, 64(6), 1926-1930 .

Sedaghat, A., Shahrestani, M .S., Noroozi, A. A., Nosratabad, A. F., Bayat, H., 2022. Developing pedotransfer functions using Sentinel-2 satellite spectral indices and Machine learning for estimating the surface soil moisture. Journal of Hydrology, 127423 .

Seo, S., 2006. A review and comparison of methods for detecting outliers in univariate data sets. University of Pittsburgh ,

SubbaNarasimha, P., Arinze, B., Anandarajan, M., 2000. The predictive accuracy of artificial neural networks and multiple regression in the case of skewed data: Exploration of some issues. Expert systems with Applications, 19(2), 117-123 .

Tietje, O., Tapkenhinrichs, M., 1993. Evaluation of pedo-transfer functions. Soil Science Society of America Journal, 57(4), 1088-1095 .

To, J., Kay, B., 2005. Variation in penetrometer resistance with soil characteristics: the contribution of effective stress and implications for pedotransfer functions. Geoderma, 126(3-4), 261-276 .

Van Genuchten, M. T., 1980. A closed-form equation for predicting the hydraulic conductivity of unsaturated soils. Soil Science Society of America Journal, 44(5), 892-898 .

Vereecken, H., Maes, J., Feyen, J., 1990. Estimating unsaturated hydraulic conductivity from easily measured soil characteristics. Soil science, 149(1), 1-12 .

Villarreal, R., Lozano, L. A., Salazar, M. P., Bellora, G. L., Melani, E. M., Polich, N., Soracco, C. G., 2020. Pore system configuration and hydraulic characteristics. Temporal variation during the crop cycle in different soil types of Argentinean Pampas Region. Soil and Tillage Research, 198, 104528 .

Wang, Y., Shao, M. a., Liu, Z., 2012. Pedotransfer functions for predicting soil hydraulic characteristics of the Chinese Loess Plateau. Soil science, 177(7), 424-432 .

Whiting, M. L., Li, L., Ustin, S. L., 2004. Predicting water content using Gaussian model on soil spectra. Remote sensing of environment, 89(4), 535-552 .

Wiermann, C., Werner, D., Horn, R., Rostek, J., Werner, B., 2000. Stress/strain processes in a structured unsaturated silty loam Luvisol under different tillage treatments in Germany. Soil and Tillage Research, 53(2), 117-128 .

Wooding, R., 1968. Steady infiltration from a shallow circular pond. Water resources research, 4(6), 1259-1273 .

Zeng, L., Shao, L., 2022. Generalized Terzaghi's Effective Stress Equation for Unsaturated Soil: An Independent Phase Balance Approach That Considers a Pore Water Content Gradient. Geofluids, 2022 .

Zhai, X., Horn, R., 2018. Effect of static and cyclic loading including spatial variation caused by vertical holes on changes in soil aeration. Soil and Tillage Research, 177, 61-67 .

Zhang, X., Wendroth, O., Matocha, C., Zhu, J., 2019. Estimating soil hydraulic conductivity at the field scale with a state-space approach. Soil science, 184(3), 101-111 .

Zhu, R., 2018. Scale and aggregate size effects on concrete fracture: Experimental investigation and discrete element modelling. École centrale de Nantes.